Heliyon 10 (2024) e38559

Contents lists available at ScienceDirect

Heliyon

journal homepage: www.cell.com/heliyon

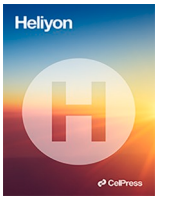

Research article

Risperidone accelerates bone loss in mice models of schizophrenia by inhibiting osteoblast autophagy

Zaihong Yang [a,1], Peifan Li [b,1], Hongyan Fan [a], Lan Pang [a], Guangyuan Xia [b], Changrong Duan [b], Lei Zheng [a,b,*]

[a] Guizhou Medical University, Guiyang, China
[b] Department of Psychiatry, Affiliated Hospital of Guizhou Medical University, Guiyang, China

ARTICLE INFO

Keywords:
Risperidone
Bone loss
Schizophrenia
Autophagy

ABSTRACT

Background: Risperidone (RIS) is the first-line drug in the clinical treatment of schizophrenia, and long-term use may lead to bone loss and even osteoporosis. This study investigated whether the mechanism of RIS-induced bone loss is related to autophagy.

Methods: The schizophrenia mice were established with the administration of MK-801. Then, RIS were injected, or autophagy inducer rapamycin (RAPA) co-injected for 8 weeks. Cognitive performance was determined by the novel object recognition and Open field tests. Bone loss of schizophrenia mice were assessed using microCT, H&E staining, ALP staining, ARS staining and WB, respectively. Autophagy of schizophrenia mice were detected by immunofluorescence, transmission electron microscopy (TEM) and WB, respectively. In addition, osteogenic differentiation of MC3T3-E1 and BMSCs cells were assessed using H&E staining, ALP staining, ARS staining and WB, respectively.

Results: In the present study, we found that RIS treatment can promote bone loss in schizophrenia mice and inhibit osteogenic differentiation of MC3T3-E1 and BMSCs cells. Interesting, the number of autophagosome and autophagy-related protein expression were decreased after RIS treatment. However, the bone loss and inhibition of osteogenic differentiation induced by RIS in schizophrenia mice were reversed by autophagy inducer RAPA.

Conclusion: RIS significantly increased bone loss and inhibited osteogenic differentiation in schizophrenia mice; the underlying mechanism entails suppressing osteoblast autophagy.

1. Introduction

Schizophrenia is a serious mental illness, the clinical symptoms mainly include delusion, hallucination, thinking disorders and so on [1,2]. Patients often have different degrees of self-control defects, and can not study, work, and live normally [3,4]. Risperidone (RIS) is one of the most widely used antipsychotics in the clinic. RIS can block the sedative effect of dopamine D2 receptor and serotonin receptor. It has the characteristics of convenient and quick drug use [5]. The study found that the risk of osteoporosis in schizophrenia was much higher than that in people with normal mental health. Patients with schizophrenia who used RIS had adverse reactions such as hyperprolactinemia, osteoporosis, and fractur [6–8]. The targeted binding of risperidone to the pituitary dopamine

* Corresponding author. Guizhou Medical University, Guiyang, China.
E-mail address: zhenglei@gmc.edu.cn (L. Zheng).
[1] These authors have contributed equally to this work.

https://doi.org/10.1016/j.heliyon.2024.e38559
Received 19 July 2024; Received in revised form 19 September 2024; Accepted 26 September 2024
Available online 27 September 2024

D2 receptor can promote the release of prolactin, and long-term hyperprolactinemia can increase the risk of osteoporosis, fracture, and even lead to breast cancer [9]. However, compared with other atypical antipsychotics, RIS did not appear to be significantly associated with an increased risk of osteoporosis [10]. Not all schizophrenic patients treated with RIS have hyperprolactinemia, and no direct evidence has been found to show that RIS, hyperprolactinemia and osteoporosis are necessarily linked. Other studies have shown that the sympathetic nervous system is also involved in RIS-induced osteoporosis [11]. Some studies have also found that RIS can inhibit osteoblast proliferation and promote osteoblast apoptosis, suggesting that risperidone can also directly act on osteocytes to cause bone metabolism disorder [12]. However, the research on the effect of RIS on bone mineral density is still very scarce, and its specific mechanism is not clear. Clarifying the mechanism of action of RIS is important for the safety of using this drug and improving the quality of life of patients.

Autophagy is a process involved in the removal of damaged cellular components or aging proteins, thereby contributing to the protection of various cells [13–15]. It maintains cell nutrition homeostasis and organelle quality control through the autophagy-lysosomal degradation pathway and participates in cell proliferation, death, differentiation, and other life processes; and, it is a potential therapeutic target for infectious diseases, neurodegeneration, cardiovascular disease, osteoporosis and many other diseases [16–18]. Previous research has demonstrated that autophagy is associated with the balance of bone metabolism and is involved in the differentiation and regulation of cell functions of mesenchymal stem cells, osteoclasts, osteoclasts [19,20]. The imbalance of cell autophagy can destroy the balance of bone remodeling and lead to bone metabolic diseases. Some autophagy-related

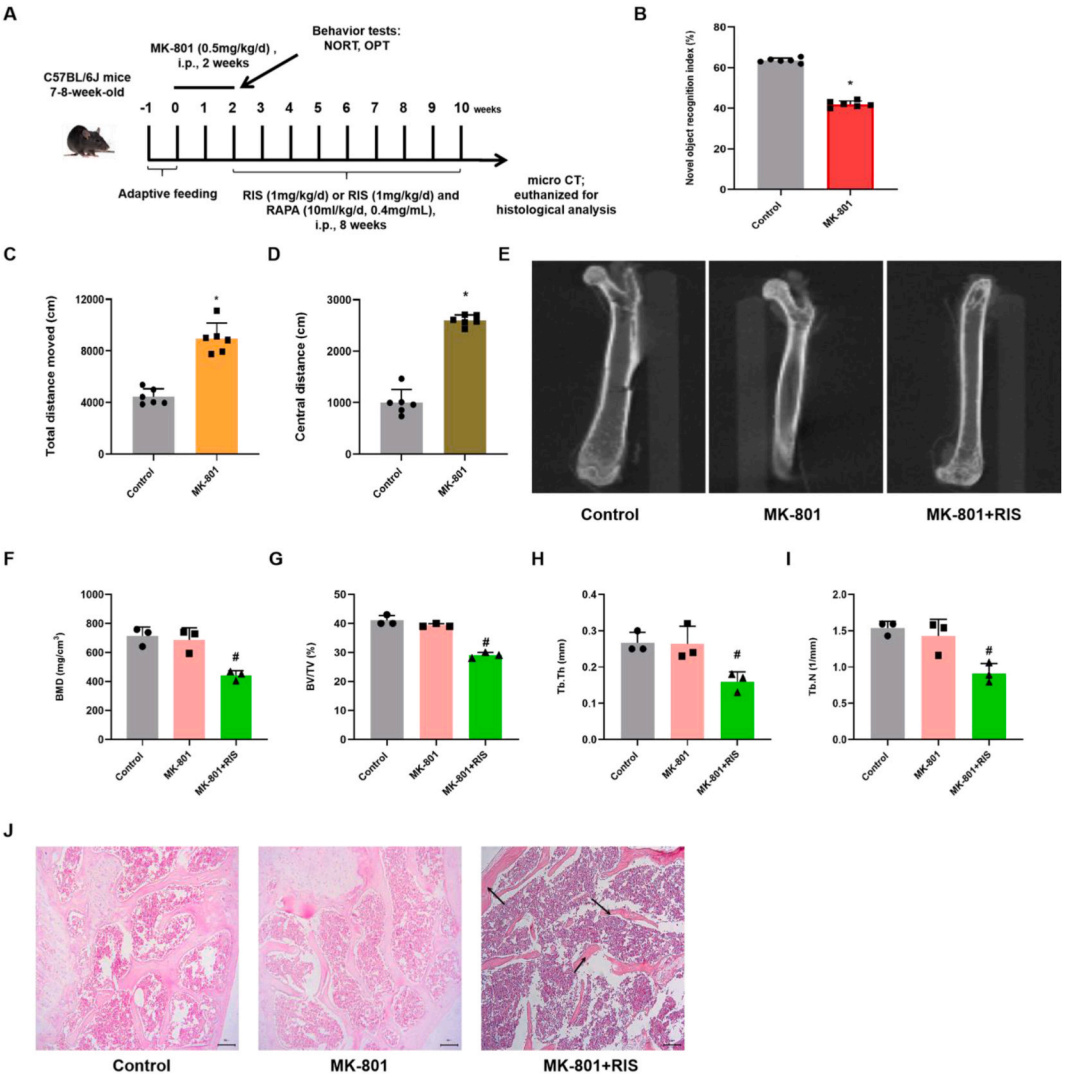

Fig. 1. Effect of RIS on bone loss in mice with schizophrenia. (**A**) A workflow of animal part experiments, **(B)** novel object recognition index, (**C-D**) open field test. The total distance moved (**C**), distance moved in central area (**D**), (**E**) representative images of microCT, **(F)** quantitative analysis of new bone formation area for bone mineral density (BMD), (**G**) directly measured bone volume fraction (BV/TV), (**H**) trabecular thickness (Tb.Th), (**I**) trabecular number (Tb.N), (**J**) H&E staining. Data are presented as the mean ± SD. *P < 0.05 vs. Control; #P < 0.05 vs. MK-801.

small-molecule drugs such as rapamycin (RAPA) and AMPK activators have been proven to be beneficial to bone regeneration [21]. Autophagy function is regulated by various mechanisms and has different effects in different cells and different environments. Zhang et al. [22] showed that risperidone can promote the expression of TNF-α, down-regulate the expression level of SATB2, further inhibit autophagy and promote apoptosis of osteoblasts. However, the specific mechanism by which risperidone regulates autophagy and affects bone metabolism is still unclear. This study aims to investigate whether risperidone causes bone loss by affecting autophagy in osteoblasts and mesenchymal stem cells.

2. Materials and methods

Materials. Mouse bone marrow mesenchymal stem cells and were MC3T3-E1 cells purchased from Wuhan Pricella Biotechnology Co., Ltd (Shanghai, China). Hematoxylin staining solution, Eosin staining solution, Alkaline phosphatase staining solution and Alizarin red staining solution were purchased from Solaibao Technology Co., LTD (Beijing, China). Antibodies against LC3 I/II, P62, Beclin-1, β-Actin, ALP, OCN and OPN were from Abcam (Cambridge, United Kingdom). Risperidone and Rapamycin were purchased from Shanghai Yuanye Bio-Technology Co., Ltd (Shanghai, China). MK-801 were purchased from MedChemExpress LLC (New Jersey, USA).

Animal model establishment and intervention. After 7 days of adaptive feeding, mice were intraperitoneally injected with MK-801 (0.5 mg/kg) for 2 weeks to establish a mouse model of schizophrenia. All experimental animal procedures were approved by the Animal Care Welfare Committee of Guizhou Medical University (permission no. 2000731). Control group mice were injected with the same amount of normal saline. The schizophrenia model was validated by a novel object recognition test and open field test. Then the MK-801 + RIS group was treated with intraperitoneal injection of RIS (1 mg/kg/d) for 8 weeks. The MK-801 + RIS + RAPA group was intraperitoneally injected with rapamycin (10 ml/kg/d, 0.4 mg/mL) after RIS injection. After 8 weeks of intervention, mice were killed by intraperitoneal injection of 0.75 % pentobarbital sodium, and femurs were collected for further examination (A workflow of animal experiments was shown in Fig. 1A).

Novel Object Recognition Test (NORT). There are three objects, A, B, and C. Objects A and B are identical, while object C is completely different from A and B. Blood glucose test paper is used for objects A and B, while cylindrical medicine bottles of similar size are used for object C. Three days before the training and testing sessions, the experimental mice were handled for 1 min each day to prevent stimulation and familiarize them with the tester. Twenty-four hours prior to the test or training session, the animals were placed in the testing room to acclimate to the environment. The two objects A and B were initially positioned at the left and right ends of a side wall during the training session. The mice were placed in the field with their backs facing the objects, ensuring that the distance between their nose tips and both objects was equal. Once the video device was activated, within 10 s, the mice were promptly introduced into the field for observation while the experimenter exited the testing room. After a duration of 10 min, they were immediately returned to their original mouse box. Following an hour of rest, object B in the field was replaced with object C while maintaining consistent positioning of the mice towards both objects. Video recording equipment was utilized throughout this process as well. The observer then left to review and record each instance when contact occurred between each mouse and either object respectively. Data on novel object recognition time, old object recognition time, as well as total time spent recognizing both novel and old objects were collected. Novel object recognition index was calculated as the following formula: novel object recognition time/total time for novel and old object recognition *100.

Open Field Test (OFT). The mouse was placed in the neutral area of the white chamber (50 cm × 50 cm × 70 cm) and given unrestricted freedom to explore for a duration of 15 min. To minimize any potential interference from odors, the box was treated with alcohol after each individual mouse.The total distance and the distance moved in the central area (cm) were measured.

Microcomputed tomography (micro-CT). Mice were euthanized under general anesthesia, and their femurs were then explanted and fixed in 4 % paraformaldehyde. The subsequent steps taken were in accordance with those described previously [23]. The three-dimensional (3D) superior aspect images and transverse views were generated using Avizo software. Micro-CT images were analyzed using PMOD 3.4 software (Pmod Technologies, Zurich, Switzerland) to calculate indexes including tissue volume (TV), bone volume (BV), directly measured bone mineral density (BMD), bone volume fraction (BV/TV), trabecular thickness (Tb.Th), and trabecular number (Tb.N).

Hematoxylin and eosin (H&E) staining. Slices were put into xylene for 15 min, washed with 100 % anhydrous ethanol for 3 min, 90 % ethanol for 3 min and 75 % ethanol for 3 min, followed by gradient ethanol dewaxing to water. Hematoxylin staining was performed for 5 min, followed by washing and soaking in PBS for 5 min, eosin staining for 2 min, washing with water, gradient alcohol dehydration, xylene treatment twice for 5 min each and neutral resin blocked cover slips. Subsequently, the femur damage were observed under an optical microscope (magnification, ×400).

Western Blotting. The total protein was extracted and the content was tested using a BCA protein assay kit. Then the protein (30 mg) was separated by 10 % SDS-PAGE and transferred onto a PVDF membrane. Membranes for target protein (and β-actin) were blocked with 5 % skimmed milk at 25 °C for 1 h. Relative membranes were incubated with primary antibody of LC3 I/II (1:1000), P62 (1:1000), Beclin-1 (1:1000), ALP (1:1000), OCN (1:1000), and OPN (1:1000),followed by incubation with secondary antibody for 1 h. Finally, the protein bands were tested by an ECL-detecting kit and β-actin was served as loading control.

Transmission electron microscopy (TEM). The femurs was dissected in order to acquire tissue samples, which were subsequently immersed in a 2.5 % solution of glutaraldehyde for a duration of 4–5 h. Following this, the samples underwent an hour-long post-fixation process utilizing a 1 % osmium tetroxide solution, followed by dehydration through a series of acetone solutions with varying concentrations and embedding in Araldite. To visualize any potential damage to mitochondrial organelles, we employed the JEM-1230 electron microscope (manufactured by JEOL, Japan).

Alkaline phosphatase (ALP) staining. Cells from each groups (1×10^6 cells) per well were plated into six-well culture plates.

Cells were then cultured for 3 days and ALP staining was performed using the alkaline phosphatase detection kit according to the manufacturer's instructions.

Alizarin red S (ARS) staining. The cell slides were removed, the remaining medium was washed with PBS, fixed with 4 % paraformaldehyde for 15 min, and then washed with PBS 3 times. According to the instructions of the kit, alizarin red staining solution was added and incubated at room temperature in the dark for 30 min, washed with distilled water, and observed by microscope.

Immunofluorescence. The cell slides were removed, and the remaining medium was washed with PBS, fixed with 4 % paraformaldehyde for 15 min, and then washed with PBS 3 times. The slides were dropped with 5%BSA and blocked at 37 °C for 30 min. A sufficient amount of diluted LC3I/II antibody (1:200) was added by dropping, and the mixture was incubated in the refrigerator at 4 °C overnight. The plates were washed three times with PBS, and the diluted cy3 fluorescent secondary antibody (1:200) was added. The plates were incubated at 37 °C for 30 min and then washed with PBS. DAPI was dropped and incubated in the dark for 3 min, excess DAPI was washed with PBS and blocked with 50 % glycerol. The images were taken under a fluorescence microscope.

Statistical Analyses. SPSS 26.0 was applied for statistical analysis, and experimental data were expressed as mean ± standard deviation (x ± s). One-Way ANOVA was used for comparison between groups, and *t*-test was selected for two-way comparison, and $P < 0.05$ was considered a statistically significant difference.

3. Results

Effect of RIS on bone loss in mice with schizophrenia. To assess the mental state of the mice injected with MK-801, NORT and OFT were performed. The results showed that compared with the control group, the novel object recognition index in the MK-801 group were significantly decreased ($P < 0.05$) (Fig. 1B). In addition, The total distance moved and distance moved in central area of the MK-801 group were significantly enhanced compared with the control group ($P < 0.05$) (Fig. 1C and D). These results suggest that the schizophrenia mice model was successfully established by MK-801. In addition, micro-CT analysis were used to evaluate bone loss of schizophrenia mice after RIS treatment (Fig. 1E). From the quantification view, BMD (Fig. 1F), BV/TV (Fig. 1G), TB.TH (Fig. 1H) and TB.N (Fig. 1I) were lower in the MK-801 + RIS group, while these parameters did not show any significant differences between the Control group and the MK-801 group. As shown in Fig. 1J, the joint surface was smooth, the tissue structure was clear, and the trabecular bone area was dense in femur tissues of both the Control group and the MK-801 group. However, bone trabecular fracture and bone loss were observed in femur tissues of mice after RIS intervention. These results indicated that RIS could induce bone loss in schizophrenic mice.

Effect of RIS on autophagy in mice with schizophrenia. To assess the effect of RIS on autophagy in mice with schizophrenia, the expression of autophagy-related proteins in femur tissues of mice was detected by WB (Fig. 2A). As shown in Fig. 2B–D, compared with the MK-801 group, the LC3 II/LC3 I and Beclin-1 protein expression in MK-801 + RIS group were significantly decreased ($P < 0.05$), while the P62 protein expression in MK-801 + RIS group were significantly increased ($P < 0.05$). In addition, TEM revealed a similar result in Fig. 2E. Compared with the MK-801 group, the number of autophagosomes in the MK-801 + RIS group were significantly decreased ($P < 0.05$). These results indicated that RIS inhibited autophagy in mice with schizophrenia.

Effect of RAPA on RIS-induced bone loss in schizophrenia mice. HE staining, ALP staining and ARS staining was used to detect

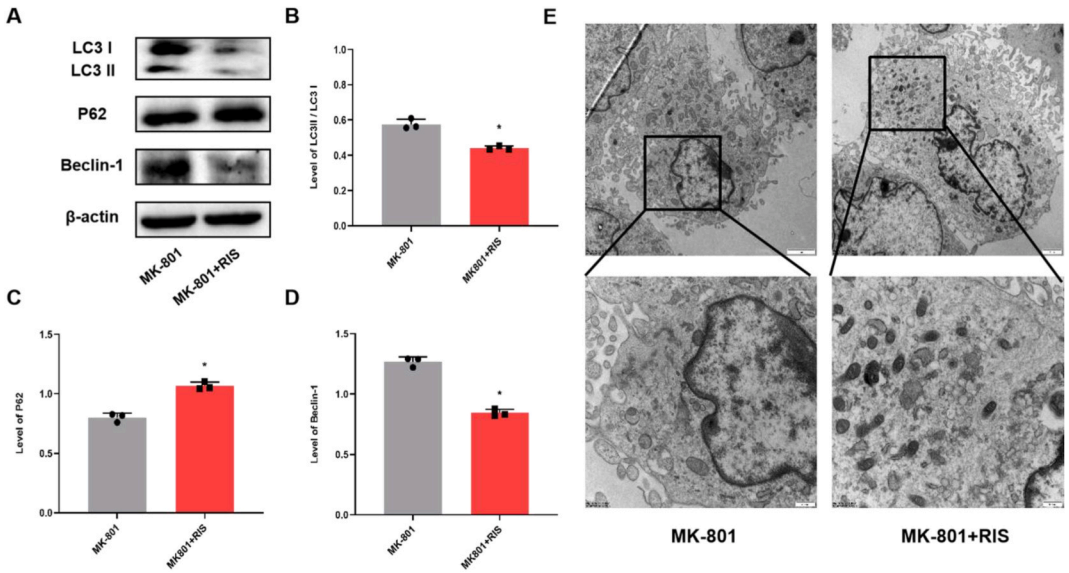

Fig. 2. Effect of RIS on autophagy in mice with schizophrenia. **(A)** autophagy-related protein expression were detected by WB, **(B-D)** quantitative analysis of autophagy-related protein expression, (**B**) LC3 I/II, (**C**) P62, (**D**) Beclin-1, **(E)** transmission electron microscopy (TEM) images. Data are presented as the mean ± SD. *$P < 0.05$ vs. MK-801 (see Supplemental Fig.s2a).

the level of bone loss in each group. As shown in Fig. 3A, the results of HE staining suggested that the trabeculae in the MK-801 + RIS group were disrupted and dissolved compared with the MK-801 group, while bone trabeculae increased in the MK-801 + RIS + RAP group. Additionally, ALP staining and ARS staining were used to detect osteoblastic differentiation in mice of each group (Fig. 3B and C). Compared with the MK-801 group, Dyeing strength, and calcium deposition in MK-801 + RIS group was significantly decreased, whereas it was increased in MK-801 + RIS + RAPA group.

As shown in Fig. 4A, immunofluorescence was used to detect the expression of LC3 I/II in mice of each group. The results showed that the level of LC3 I/II was significantly reduced in the MK-801 + RIS group compared to the MK-801 group. Compared with the MK-801 + RIS group, the LC3 I/II protein expression in the MK-801 + RIS + RAPA group were significantly increased. However, the expression of osteogenic related proteins in femur tissues of mice was detected by WB (Fig. 4B). As shown in Fig. 4C–E, the ALP, OCN, and OPN protein expression in the MK-801 + RIS group were significantly decreased compared with the MK-801 group ($P < 0.05$), while it was significantly increased in the MK-801 + RIS + RAPA group compared with the MK-801 + RIS group ($P < 0.05$). These results suggest that RIS can induce bone loss in schizophrenia mice by inhibiting autophagy.

RAPA treatment reverses the inhibitory effect of RIS on autophagy in MC3T3-E1 cells. A workflow of experiments in MC3T3-E1 cells was shown in Fig. 5A. To investigate whether RIS affects the autophagy of MC3T3-E1 cells, the cells were treated with 3 μM RAPA for 48 h to explore the effect of RIS on autophagy in MC3T3-E1 cells. The results of TEM revealed that compared with the Control group, the number of autophagosomes in the RIS group were significantly decreased. Compared with the RIS group, the number of autophagosomes were significantly increased after RAPA treatment (Fig. 5B). In addition, immunofluorescence was used to detect the expression of LC3 I/II in MC3T3-E1 cells (Fig. 5C). The results showed that the level of LC3 I/II was significantly reduced in the RIS group compared to the control group. Compared with the RIS group, the LC3 I/II protein expression in the RIS + RAPA group were significantly increased. These results indicated that RAPA treatment reverses the inhibitory effect of RIS on autophagy in MC3T3-E1 cells.

RAPA treatment reverses the inhibitory effect of RIS on osteogenesis in MC3T3-E1 cells. ALP staining and ARS staining were used to detect the osteogenic effect of each group on MC3T3-E1 cells (Fig. 6A and B). Compared with the control group, Dyeing strength, and calcium deposition in RIS group was significantly decreased, whereas it was increased in the RIS + RAPA group. However, the expression of osteogenic related proteins in MC3T3-E1 cells was detected by WB (Fig. 6C). As shown in Fig. 6D, the ALP, OCN, and OPN protein expression in the RIS group were significantly decreased compared with the control group ($P < 0.05$), while it was significantly increased in the RIS + RAPA group compared with the RIS group ($P < 0.05$). These results suggest that RIS can inhibit osteogenesis in MC3T3-E1 cells by inhibiting autophagy.

Osteogenic differentiation of BMSCs were inhibited by RIS through autophagy. A workflow of experiments in BMSCs was shown in Fig. 7A. The effect of RIS on the osteogenic differentiation of mouse BMSCS was further investigated, and the results are

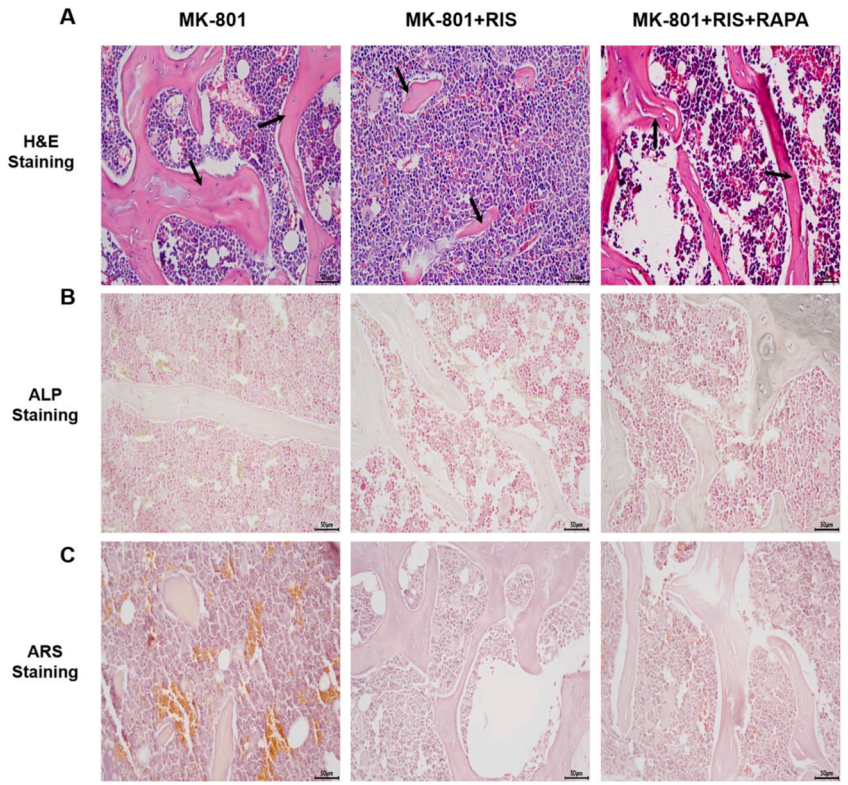

Fig. 3. Detection of bone loss by pathological staining. (**A**) H&E staining, (**B**) ALP staining, (**C**) ARS staining.

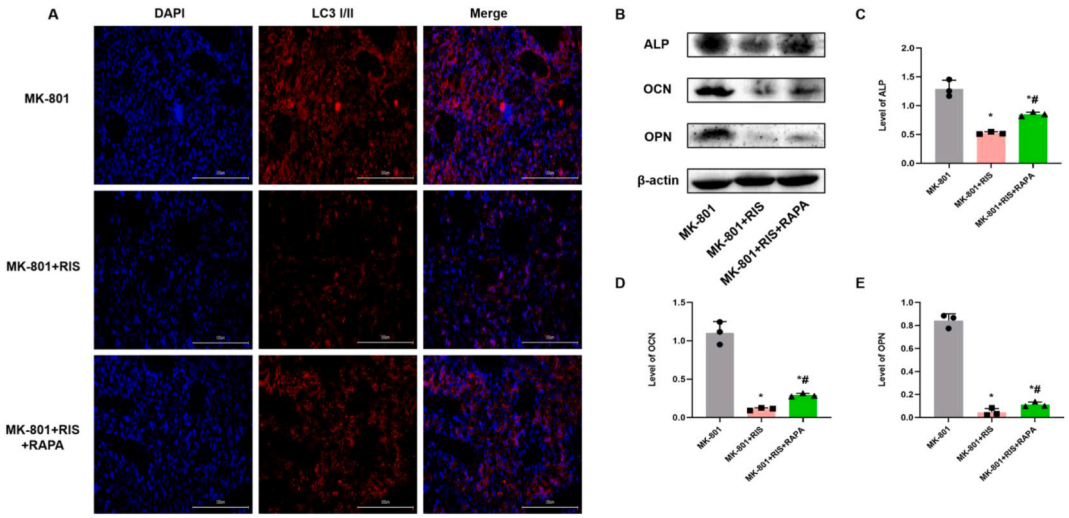

Fig. 4. Effect of RAPA on RIS-induced bone loss in schizophrenia mice. (**A**) LC3 I/II protein expression results were detected by immunofluorescence, (**B**) osteogenic-related protein expression were detected by WB, **(C-E)** quantitative analysis of osteogenic-related protein expression, (**C**) ALP, (**D**) OCN, (**E**) OPN. Data are presented as the mean ± SD. *P < 0.05 vs. MK-801; #P < 0.05 vs. MK-8011 + RIS (see Supplemental Fig.s4b).

shown below. As shown in Fig. 7B, the expression of LC3 I/II, P62, Beclin-1, ALP, OCN and OPN proteins in BMSCs was detected by WB. Compared with the control group, the LC3 II/LC3 I, Beclin-1, ALP, OCN, and OPN protein expression in the RIS group were significantly decreased compared with the control group ($P < 0.05$), while the P62 protein expression in RIS group were significantly increased ($P < 0.05$) (Fig. 7C–H). However, ALP staining and ARS staining were further used to detect the osteogenic effect of RIS and RAPA on BMSCs (Fig. 7I and J). Compared with the control group, Dyeing strength, and calcium deposition in RIS group was significantly decreased, whereas it was increased in the RIS + RAPA group. To further investigate whether RIS affects the autophagy of BMSCs, the expression of osteogenic related proteins in BMSCs was detected by WB (Fig. 7K). As shown in Fig. 7L, compared with the RIS group, RAPA treatment significantly increased the ALP, OCN, and OPN protein expression in BMSCs ($P < 0.05$). These results indicated that RIS inhibited the osteogenic differentiation of BMSC cells by inhibiting autophagy.

4. Discussion

Risperidone (RIS) is one of the first-line anti-schizophrenia drugs in clinic. However, more and more studies have shown that RIS and other anti-schizophrenic drugs are closely related to bone loss in patients [24–26]. As many as two-thirds of patients treated with atypical anti-schizophrenic drugs have impaired bone mineral density, and likelihood of fracture was positively correlated with this kind of drug [27]. A variety of antipsychotic drugs can promote osteoblast apoptosis and lead to osteoporosis through the Wnt/β-catenin signaling pathway [28]. However, the specific sub-regulatory mechanism of risperidone induced bone mass loss is still unclear, and understanding its mechanism of action is important for the medication management of schizophrenia patients. We used MK-801 to induce the schizophrenia mice model. After 8 weeks of RIS treatment, the mice developed osteoporosis symptoms, with a large number of fractured and absent trabecular bone. Consistent with this, studies have shown that risperidone can directly act on MC3T3-E1 cells to inhibit cell proliferation and promote apoptosis, which in turn leads to the occurrence of osteoporosis.

Bone metabolism is achieved through bone formation and bone resorption involving osteoblasts and osteoclasts, and its metabolic activity is a dynamic balance process. The destruction of bone metabolic balance caused by functional changes in osteoblasts and osteoclasts is one of the main factors of osteoporosis [29,30]. In addition, stem cells also play an important role in bone reconstruction. Mesenchymal stem cells have been attracting much attention due to their good differentiation ability and strong immunomodulatory activity. Mesenchymal stem cells have multipotent differentiation potential, can migrate to the damaged site to promote tissue regeneration, and have shown good therapeutic effects in degenerative diseases [31–33]. We also investigated the effect of RIS on MC3T3-E1 cells and BMSCs in vitro. The results showed that RIS inhibited the expression of ALP, OCN, OPN, and calcium deposition in MC3T3-E1 cells. In addition, RIS could not only directly inhibit the bone formation of osteoblasts, but also reduce bone formation leading to osteoporosis by inhibiting the osteogenic differentiation of BMSCs.

To explore the mechanism of RIS regulating the osteogenic differentiation of BMSC, we observed that the amount of autophagosomes in MC3T3-E1 cells was significantly reduced after RIS treatment by TEM. Then we have observed that the expression changes of autophagy-related proteins in MC3T3-E1 cells and BMSC cells after RIS treatment by WB. The results showed that the levels of LC3II/LC3I and Beclin-1 were decreased and the expression of P62 was increased in both cells after RIS treatment, indicating that RIS could inhibit the level of autophagy in osteoblasts and BMSC. Autophagy is an important process for cells to maintain cell homeostasis in the process of proliferation, differentiation, and maturation. It participates in various cellular processes by degrading misfolded or aggregated proteins, damaged organelles, or macromolecules in the cytoplasm, and has become a potential target for the prevention

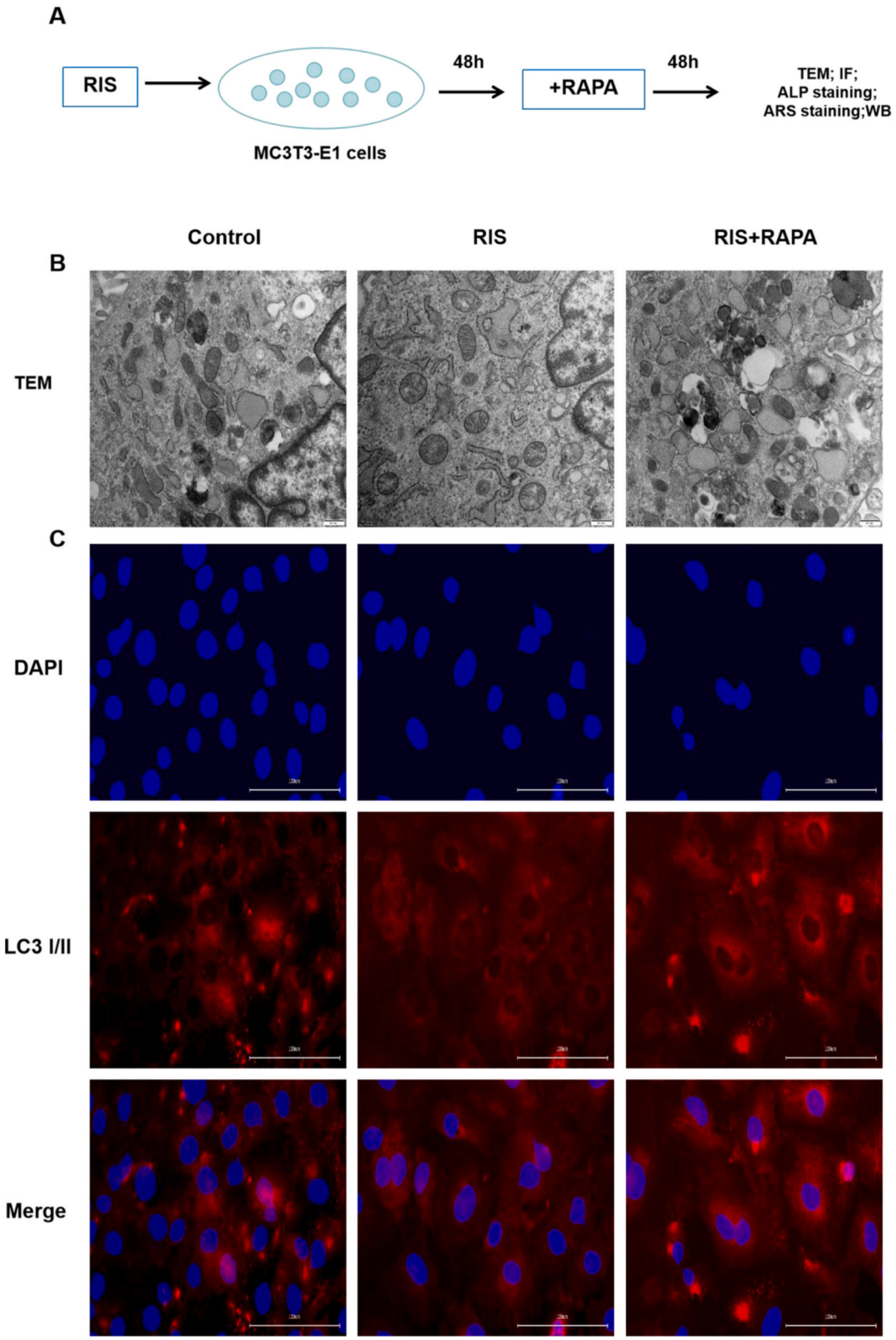

Fig. 5. RAPA treatment reverses the inhibitory effect of RIS on autophagy in MC3T3-E1 cells. (**A**) A workflow of experiments was conducted in MC3T3-E1 cells, **(B)** autophagosomes were observed by TEM, **(C)** LC3 I/II protein expression results were detected by immunofluorescence.

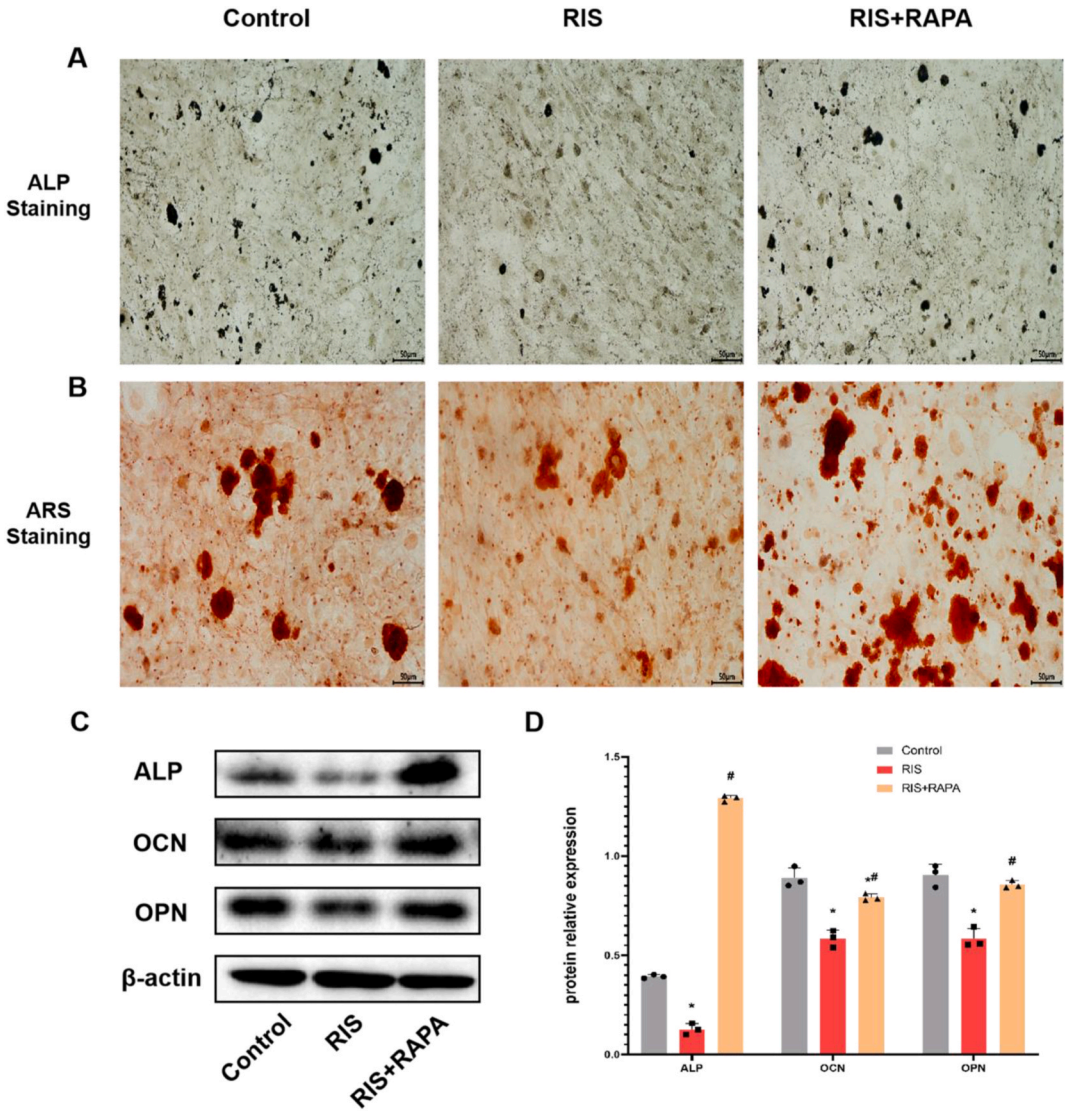

Fig. 6. RAPA treatment reverses the inhibitory effect of RIS on osteogenesis in MC3T3-E1 cells. (**A**) ALP staining, (**B**) ARS staining, (**C-D**) ALP,OCN and OPN protein expression were detected by WB. Data are presented as the mean ± SD. *P < 0.05 vs. Control; #P < 0.05 vs. RIS (see Supplemental Fig.s6c).

and treatment of osteoporosis [34–36]. Autophagy is a process tightly regulated by intrinsic molecules. After autophagy activation, Beclin 1 is phosphorylated by ULK1 to promote the localization of autophagy proteins to autophagic vesicles. Under the action of ATG7 and ATG3 enzymes, LC3 I covalently binds to phosphatidylethanolamine (PE) to form membrane-binding protein LC3-II, which binds to the autophagosome membrane and participates in autophagosome membrane formation. Subsequently, SQSTM-1/p62 transported the ubiquitinated proteins to the autophagosome to promote the degradation of substances inside the autophagosome [37–40]. To further verify the relationship between RIS and autophagy, we used autophagy inducer rapamycin (RAPA) to treat cells, and the results showed that RAPA could increase the level of autophagy in RIS treated MC3T3-E1 cells and BMSC cells. Reverse the inhibitory effect of RIS on ALP, OCN, OPN expression, and osteogenic differentiation of BMSC. We then validated this in animals where RIS induced bone mass loss could be alleviated by the administration of RAPA. Taken together, our results suggest that inhibition of autophagy by RIS inhibits both MC3T3-E1 cells and BMSCs osteogenic differentiation, thereby disrupting the balance of bone metabolism and leading to osteoporosis. However, this study also has some limitations. As we all know, autophagy is influenced by various signaling pathways. Although our study found that RIS can inhibit autophagy in osteoblasts, it remains unclear which specific signaling pathway risperidone targets to inhibit autophagy in osteoblasts. In subsequent studies, we will further investigate the specific signaling pathway involved in risperidone's regulation of osteoblast autophagy.

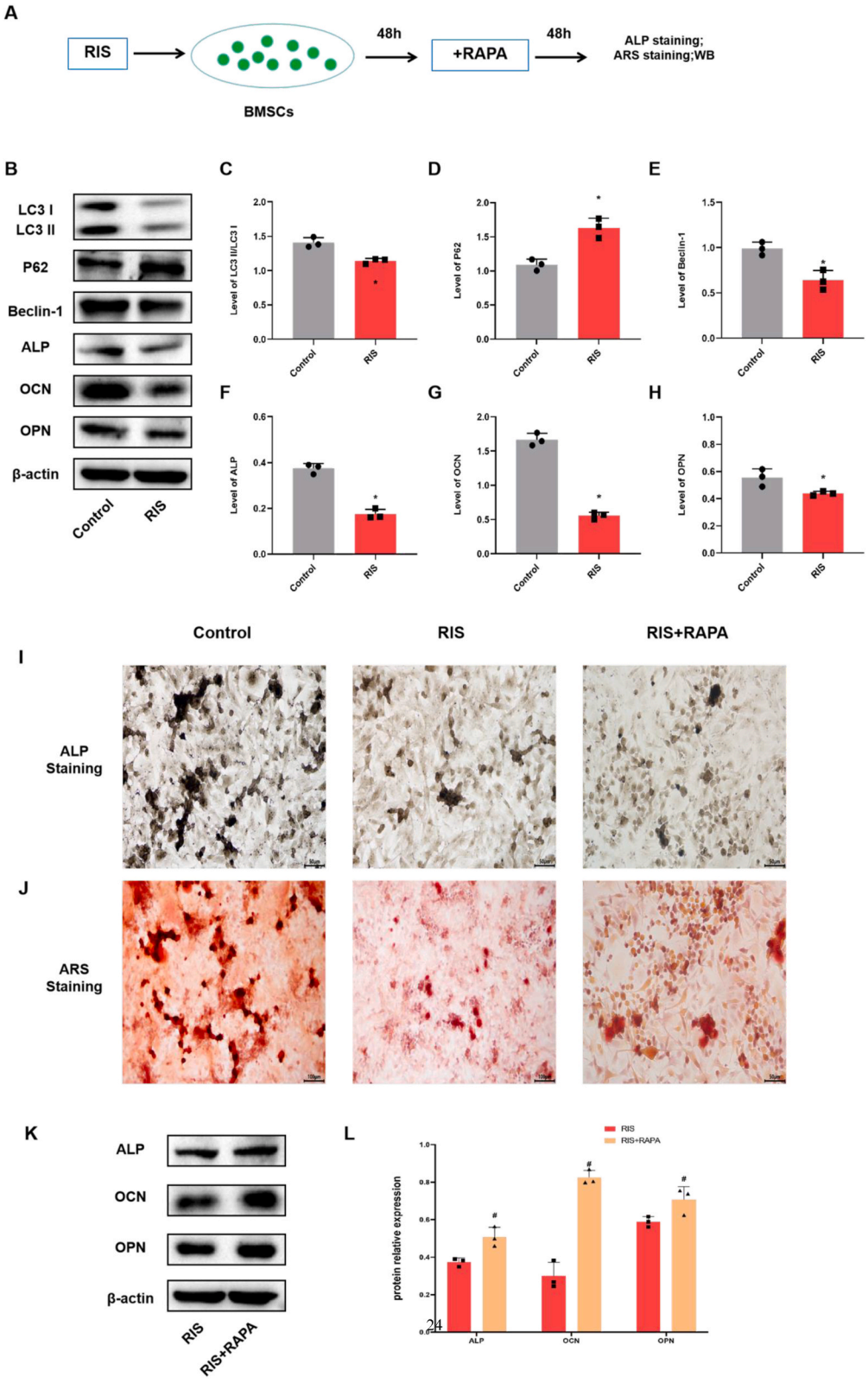

(caption on next page)

Fig. 7. Osteogenic differentiation of BMSCs were inhibited by RIS through autophagy. (**A**) A workflow of experiments was conducted in BMSCs, (**B**) protein expression were detected by WB, (**C-H**) quantitative analysis of protein expression, (**B**) LC3 I/II, (**C**) P62, (**D**) Beclin-1,(**E**) ALP, (**F**) OCN, (**G**) OPN, (**I**) ALP staining, (**J**) ARS staining, (**K-L**) ALP,OCN and OPN protein expression were detected by WB. Data are presented as the mean ± SD. *P < 0.05 vs. Control; #P < 0.05 vs. RIS (see Supplemental Fig.s7b, Fig.s7k).

5. Conclusions

Based upon the results of the present study, we conclude that RIS can inhibits both MC3T3-E1 cells and BMSCs osteogenic differentiation by inhibiting autophagy, which further induce bone loss in schizophrenia mice.

Data availability statement

Data will be made available on request.

Funding

This research was supported by grants from the National Natural Science Foundation of China [grant numbers:82060651] and the Doctoral Research Fund of Affiliated Hospital of Guizhou Medical University [grant numbers: GYFYBSKY-2021-67].

CRediT authorship contribution statement

Zaihong Yang: Writing – original draft, Project administration, Methodology, Data curation. **Peifan Li:** Writing – original draft, Software, Project administration, Methodology. **Hongyan Fan:** Visualization, Validation, Data curation. **Lan Pang:** Software, Project administration, Formal analysis. **Guangyuan Xia:** Supervision, Software, Methodology. **Changrong Duan:** Writing – review & editing, Project administration, Methodology, Investigation. **Lei Zheng:** Writing – review & editing, Funding acquisition, Data curation.

Declaration of competing interest

The authors declare that they have no known competing financial interests or personal relationships that could have appeared to influence the work reported in this paper.

Appendix A. Supplementary data

Supplementary data to this article can be found online at https://doi.org/10.1016/j.heliyon.2024.e38559.

References

[1] R.E. Lawrence, A. Bernstein, Schizophrenia and emergency medicine, Emerg. Med. Clin. 42 (2024) 93–104, https://doi.org/10.1016/j.emc.2023.06.012.
[2] V. Gallese, M. Ardizzi, F. Ferroni, Schizophrenia and the bodily self, Schizophr. Res. 269 (2024) 152–162, https://doi.org/10.1016/j.schres.2024.05.014.
[3] S.S. Gangadin, A.D. Enthoven, N.J.M. van Beveren, J.D. Laman, I.E.C. Sommer, Immune dysfunction in schizophrenia spectrum disorders, Annu. Rev. Clin. Psychol. 20 (2024) 229–257, https://doi.org/10.1146/annurev-clinpsy-081122-013201.
[4] L. Sass, J. Feyaerts, Schizophrenia, the very idea: on self-disorder, hyperreflexivity, and the diagnostic concept, Schizophr. Res. 267 (2024) 473–486, https://doi.org/10.1016/j.schres.2024.03.022.
[5] J.M. Kane, E. Harary, R. Eshet, O. Tohami, M. Weiser, S. Leucht, A. Merenlender-Wagner, N. Sharon, G.L.3rd Davis, M. Suett, K.R. Franzenburg, C.U. Correll, Efficacy and safety of TV-46000, a long-acting, subcutaneous, injectable formulation of risperidone, for schizophrenia: a randomised clinical trial in the USA and Bulgaria, Lancet Psychiatr. 10 (2023) 934–943, https://doi.org/10.1016/S2215-0366(23)00288-2.
[6] M.A. Ramos-Méndez, C.A. Tovilla-Zárate, I.E. Juárez-Rojop, M. Villar-Soto, A.D. Genis-Mendoza, T.B. González-Castro, M.L. López-Narváez, J.J. Martínez-Magaña, R.G. Castillo-Avila, G.E. Villar-Juárez, Effect of risperidone on serum IL-6 levels in individuals with schizophrenia: a systematic review and meta-analysis, Int. J. Psychiatr. Clin. Pract. 27 (2023) 171–178, https://doi.org/10.1080/13651501.2022.2100264.
[7] C. Álamo, Risperidone ism as a new option in the clinical management of schizophrenia: a narrative review, Adv. Ther. 39 (2022) 4875–4891, https://doi.org/10.1007/s12325-022-02299-8.
[8] A. Shamabadi, S. Fattollahzadeh-Noor, B. Fallahpour, F.A. Basti, M.R. Khodaei Ardakani, S. Akhondzadeh, L-Theanine adjunct to risperidone in the treatment of chronic schizophrenia inpatients: a randomized, double-blind, placebo-controlled clinical trial, Psychopharmacology (Berl). 240 (2023) 2631–2640, https://doi.org/10.1007/s00213-023-06458-9.
[9] C. Bushe, M. Shaw, R.C. Peveler, A review of the association between antipsychotic use and hyperprolactinaemia, J. Psychopharmacol. 22 (2008) 46–55, https://doi.org/10.1177/0269881107088435.
[10] E. Clapham, R. Bodén, J. Reutfors, T. Svensson, D. Ramcharran, H. Qiu, H. Kieler, S. Bahmanyar, Exposure to risperidone versus other antipsychotics and risk of osteoporosis-related fractures: a population-based study, Acta Psychiatr. Scand. 141 (2020) 74–83, https://doi.org/10.1111/acps.13101.
[11] K.J. Motyl, M. Beauchemin, D. Barlow, P.T. Le, K. Nagano, A. Treyball, A. Contractor, R. Baron, C.J. Rosen, K.L. Houseknecht, A novel role for dopamine signaling in the pathogenesis of bone loss from the atypical antipsychotic drug risperidone in female mice, Bone 103 (2017) 168–176, https://doi.org/10.1016/j.bone.2017.07.008.
[12] L. Zheng, L. Yang, X. Zhao, N. Long, P. Li, Y. Wang, Effect of risperidone on proliferation and apoptosis of MC3T3-E1 cells, Braz. J. Med. Biol. Res. 52 (2019) e8098, https://doi.org/10.1590/1414-431X20188098.

[13] Y. Chen, J. Chen, Z. Xing, C. Peng, D. Li, Autophagy in neuroinflammation: a focus on epigenetic regulation, Aging Dis 15 (2024) 739–754, https://doi.org/10.14336/AD.2023.0718-1.
[14] Y. Tang, W. Xu, Y. Liu, J. Zhou, K. Cui, Y. Chen, Autophagy protects mitochondrial health in heart failure, Heart Fail. Rev. 29 (2024) 113–123, https://doi.org/10.1007/s10741-023-10354-x.
[15] J.N. Shang, C.G. Yu, R. Li, Y. Xi, Y.J. Jian, N. Xu, S. Chen, The nonautophagic functions of autophagy-related proteins, Autophagy 20 (2024) 720–734, https://doi.org/10.1080/15548627.2023.2254664.
[16] J.A. Pavlova, E.A. Guseva, O.A. Dontsova, P.V. Sergiev, Natural activators of autophagy, Biochemistry (Mosc). 89 (2024) 1–26, https://doi.org/10.1134/S0006297924010012.
[17] B.A. Marzoog, Autophagy behavior in endothelial cell regeneration, Curr. Aging Sci. 17 (2024) 58–67, https://doi.org/10.2174/0118746098260689231002044435.
[18] Y.Y. Li, Z.H. Qin, R. Sheng, The multiple roles of autophagy in neural function and diseases, Neurosci. Bull. 40 (2024) 363–382, https://doi.org/10.1007/s12264-023-01120-y.
[19] M. Borsa, S. Obba, F.C. Richter, H. Zhang, T. Riffelmacher, J. Carrelha, G. Alsaleh, S.E.W. Jacobsen, A.K. Simon, Autophagy preserves hematopoietic stem cells by restraining MTORC1-mediated cellular anabolism, Autophagy 20 (2024) 45–57, https://doi.org/10.1080/15548627.2023.2247310.
[20] H. Yao, L. Xiang, Y. Huang, J. Tan, Y. Shen, F. Li, F. Geng, W. Liu, X. Li, Y. Gao, Guizhi Shaoyao Zhimu granules attenuate bone destruction in mice with collagen-induced arthritis by promoting mitophagy of osteoclast precursors to inhibit osteoclastogenesis, Phytomedicine 118 (2023) 154967, https://doi.org/10.1016/j.phymed.2023.154967.
[21] J. Wang, Y. Zhang, J. Cao, Y. Wang, N. Anwar, Z. Zhang, D. Zhang, Y. Ma, Y. Xiao, L. Xiao, X. Wang, The role of autophagy in bone metabolism and clinical significance, Autophagy 19 (2023) 2409–2427, https://doi.org/10.1080/15548627.2023.2186112.
[22] S. Zhang, W. He, A. Li, C. Zhao, Y. Chen, C. Xu, Q. Zhang, D. Zheng, M. Chen, H. Miao, Y. Huang, Involvement of the TNF-α/SATB2 axis in the induced apoptosis and inhibited autophagy of osteoblasts by the antipsychotic Risperidone, Mol. Med. 28 (2022) 46, https://doi.org/10.1186/s10020-022-00466-9.
[23] K. Kerschan-Schindl, M. Papageorgiou, U. Föger-Samwald, M. Butylina, M. Weber, P. Pietschmann, Assessment of bone microstructure by micro CT in C57bl/6J mice for sex-specific differentiation, Int. J. Mol. Sci. 23 (2022) 14585, https://doi.org/10.3390/ijms232314585.
[24] R. Chenniappan, H. Nandeesha, S. Kattimani, A.C. Goud, D. Thiagarajan, Risperidone reduces matrix metalloproteinase-9 and increases neurotrophin-3 in schizophrenia spectrum of disorder, Indian J. Clin. Biochem. 37 (2022) 342–348, https://doi.org/10.1007/s12291-021-00985-y.
[25] M. Hu, Y. Xia, X. Zong, J.A. Sweeney, J.R. Bishop, Y. Liao, G. Giase, B. Li, L.H. Rubin, Y. Wang, Z. Li, Y. He, X. Chen, C. Liu, C. Chen, J. Tang, Risperidone-induced changes in DNA methylation in peripheral blood from first-episode schizophrenia patients parallel changes in neuroimaging and cognitive phenotypes, Psychiatr. Res. 317 (2022) 114789, https://doi.org/10.1016/j.psychres.2022.114789.
[26] E. Bellotti, G. Contarini, F. Geraci, S.A. Torrisi, C. Piazza, F. Drago, G.M. Leggio, F. Papaleo, P. Decuzzi, Long-lasting rescue of schizophrenia-relevant cognitive impairments via risperidone-loaded microPlates, Drug Deliv Transl Res 12 (2022) 1829–1842, https://doi.org/10.1007/s13346-021-01099-x.
[27] N.C. Anastasio, K.M. Johnson, Atypical anti-schizophrenic drugs prevent changes in cortical N-methyl-D-aspartate receptors and behavior following sub-chronic phencyclidine administration in developing rat pups, Pharmacol. Biochem. Behav. 90 (2008) 569–577, https://doi.org/10.1016/j.pbb.2008.04.017.
[28] P. Li, Y. Wang, X. Liu, Z. Zhou, J. Wang, H. Zhou, L. Zheng, L. Yang, Atypical antipsychotics induce human osteoblasts apoptosis via Wnt/β-catenin signaling, BMC Pharmacol Toxicol 20 (2019) 10, https://doi.org/10.1186/s40360-019-0287-9.
[29] J.M. Kim, C. Lin, Z. Stavre, M.B. Greenblatt, J.H. Shim, Osteoblast-Osteoclast communication and bone homeostasis, Cells 9 (2020) 2073, https://doi.org/10.3390/cells9092073.
[30] A.J. Donaubauer, L. Deloch, I. Becker, R. Fietkau, B. Frey, U.S. Gaipl, The influence of radiation on bone and bone cells-differential effects on osteoclasts and osteoblasts, Int. J. Mol. Sci. 21 (2020) 6377, https://doi.org/10.3390/ijms21176377.
[31] R. Margiana, A. Markov, A.O. Zekiy, M.U. Hamza, K.A. Al-Dabbagh, S.H. Al-Zubaidi, N.M. Hameed, I. Ahmad, R. Sivaraman, H.H. Kzar, M.E. Al-Gazally, Y. F. Mustafa, H. Siahmansouri, Clinical application of mesenchymal stem cell in regenerative medicine: a narrative review, Stem Cell Res. Ther. 13 (2022) 366, https://doi.org/10.1186/s13287-022-03054-0.
[32] A. Naji, M. Eitoku, B. Favier, F. Deschaseaux, N. Rouas-Freiss, N. Suganuma, Biological functions of mesenchymal stem cells and clinical implications, Cell. Mol. Life Sci. 76 (2019) 3323–3348, https://doi.org/10.1007/s00018-019-03125-1.
[33] X. Zhang, W. Jiang, C. Xie, X. Wu, Q. Ren, F. Wang, X. Shen, Y. Hong, H. Wu, Y. Liao, Y. Zhang, R. Liang, W. Sun, Y. Gu, T. Zhang, Y. Chen, W. Wei, S. Zhang, W. Zou, H. Ouyang, Msx1+ stem cells recruited by bioactive tissue engineering graft for bone regeneration, Nat. Commun. 13 (2022) 5211, https://doi.org/10.1038/s41467-022-32868-y.
[34] M. Shariq, N. Quadir, A. Alam, S. Zarin, J.A. Sheikh, N. Sharma, J. Samal, U. Ahmad, I. Kumari, S.E. Hasnain, N.Z. Ehtesham, The exploitation of host autophagy and ubiquitin machinery by Mycobacterium tuberculosis in shaping immune responses and host defense during infection, Autophagy 19 (2023) 3–23, https://doi.org/10.1080/15548627.2021.2021495.
[35] G.R. Golovkine, A.W. Roberts, H.M. Morrison, R. Rivera-Lugo, R.M. McCall, H. Nilsson, N.E. Garelis, T. Repasy, M. Cronce, J. Budzik, E. Van Dis, L.M. Popov, G. Mitchell, R. Zalpuri, D. Jorgens, J.S. Cox, Autophagy restricts Mycobacterium tuberculosis during acute infection in mice, Nat Microbiol 8 (2023) 819–832, https://doi.org/10.1038/s41564-023-01354-6.
[36] S. Nasrah, A. Radi, J.K. Daberkow, H. Hummler, S. Weber, E. Seaayfan, M. Kömhoff, MAGED2 depletion promotes stress-induced autophagy by impairing the cAMP/PKA pathway, Int. J. Mol. Sci. 24 (2023) 13433, https://doi.org/10.3390/ijms241713433.
[37] H. Yamamoto, T. Matsui, Molecular mechanisms of macroautophagy, microautophagy, and chaperone-mediated autophagy, J. Nippon Med. Sch. 91 (2024) 2–9, https://doi.org/10.1272/jnms.JNMS.2024_91-102.
[38] C. Dou, Y. Zhang, L. Zhang, C. Qin, Autophagy and autophagy-related molecules in neurodegenerative diseases, Animal Model Exp Med 6 (2023) 10–17, https://doi.org/10.1002/ame2.12229.
[39] D. Bhatia, M.E. Choi, Autophagy and mitophagy: physiological implications in kidney inflammation and diseases, Am. J. Physiol. Ren. Physiol. 325 (2023) F1–F21, https://doi.org/10.1152/ajprenal.00012.2023.
[40] Y. Hama, Y. Ogasawara, N.N. Noda, Autophagy and cancer: basic mechanisms and inhibitor development, Cancer Sci. 114 (2023) 2699–2708, https://doi.org/10.1111/cas.15803.